



Istituto Nazionale di Astrofisica

Osservatorio Astronomico di Brera

# Short GRB properties and rate in the Gravitational Wave era

Paolo D'Avanzo

INAF – Osservatorio Astronomico di Brera

and: **G. Ghirlanda**, O.S. Salafia, A. Pescali, G. Ghisellini, R. Salvaterra, E. Chassande-Mottin, M. Colpi, F. Nappo,, A. Melandri, M. G. Bernardini, M. Branchesi, S. Campana R. Ciolfi, S. Covino, D. Gotz, S. D. Vergani, M. Zennaro, G. Tagliaferri

Astronomy & Astrophysics in press (arXiv: 1607.07875)

# The GW era



PRL 116, 061102 (2016)

Selected for a Viewpoint in *Physics*  
PHYSICAL REVIEW LETTERS

week ending  
12 FEBRUARY 2016



## Observation of Gravitational Waves from a Binary Black Hole Merger

B. P. Abbott *et al.*\*

(LIGO Scientific Collaboration and Virgo Collaboration)

(Received 21 January 2016; published 11 February 2016)

On September 14, 2015 at 09:50:45 UTC the two detectors of the Laser Interferometer Gravitational-Wave Observatory simultaneously observed a transient gravitational-wave signal. The signal sweeps upwards in frequency from 35 to 250 Hz with a peak gravitational-wave strain of  $1.0 \times 10^{-21}$ . It matches the waveform predicted by general relativity for the inspiral and merger of a pair of black holes and the ringdown of the resulting single black hole. The signal was observed with a matched-filter signal-to-noise ratio of 24 and a false alarm rate estimated to be less than 1 event per 203 000 years, equivalent to a significance greater than  $5.1\sigma$ . The source lies at a luminosity distance of  $410_{-180}^{+160}$  Mpc corresponding to a redshift  $z = 0.09_{-0.04}^{+0.03}$ . In the source frame, the initial black hole masses are  $36_{-4}^{+5} M_{\odot}$  and  $29_{-4}^{+4} M_{\odot}$ , and the final black hole mass is  $62_{-4}^{+4} M_{\odot}$ , with  $3.0_{-0.5}^{+0.5} M_{\odot} c^2$  radiated in gravitational waves. All uncertainties define 90% credible intervals. These observations demonstrate the existence of binary stellar-mass black hole systems. This is the first direct detection of gravitational waves and the first observation of a binary black hole merger.

DOI: 10.1103/PhysRevLett.116.061102

# The GW era



Selected for a **Viewpoint** in *Physics*  
 PHYSICAL REVIEW LETTERS  
 PRL 116, 061102 (2016) week ending 12 FEBRUARY 2016



## Observation of Gravitational Waves from a Binary Black Hole Merger

B. P. Abbott *et al.*\*

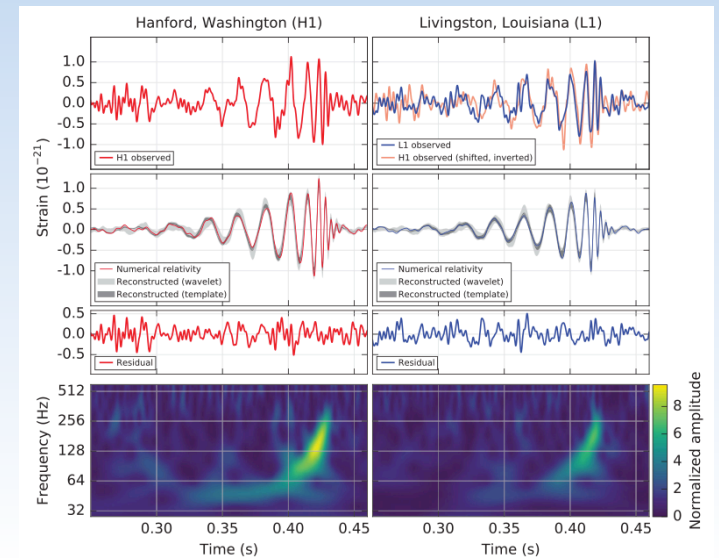
(LIGO Scientific Collaboration and Virgo Collaboration)

(Received 21 January 2016; published 11 February 2016)

On September 14, 2015 at 09:50:45 UTC the two detectors of the Laser Interferometer Gravitational-Wave Observatory simultaneously observed a transient gravitational-wave signal. The signal sweeps upwards in frequency from 35 to 250 Hz with a peak gravitational-wave strain of  $1.0 \times 10^{-21}$ . It matches the waveform predicted by general relativity for the inspiral and merger of a pair of black holes and the ringdown of the resulting single black hole. The signal was observed with a matched-filter signal-to-noise ratio of 24 and a false alarm rate estimated to be less than 1 event per 203 000 years, equivalent to a significance greater than  $5.1\sigma$ . The source lies at a luminosity distance of  $410^{+160}_{-180}$  Mpc corresponding to a redshift  $z = 0.09^{+0.03}_{-0.04}$ . In the source frame, the initial black hole masses are  $36^{+5}_{-4} M_{\odot}$  and  $29^{+4}_{-4} M_{\odot}$ , and the final black hole mass is  $62^{+4}_{-4} M_{\odot}$ , with  $3.0^{+0.5}_{-0.5} M_{\odot} c^2$  radiated in gravitational waves. All uncertainties define 90% credible intervals. These observations demonstrate the existence of binary stellar-mass black hole systems. This is the first direct detection of gravitational waves and the first observation of a binary black hole merger.

DOI: 10.1103/PhysRevLett.116.061102

Primary black hole mass	$36^{+5}_{-4} M_{\odot}$
Secondary black hole mass	$29^{+4}_{-4} M_{\odot}$
Final black hole mass	$62^{+4}_{-4} M_{\odot}$
Final black hole spin	$0.67^{+0.05}_{-0.07}$
Luminosity distance	$410^{+160}_{-180}$ Mpc
Source redshift $z$	$0.09^{+0.03}_{-0.04}$



# The GW era – O1



## Sept 2015 – Jan 2016: LVC O1 science run

2 high-significance ( $\text{FAR} < 1/\text{century}$ ) GW events during O1 (GW 150914, GW 151226)  
+ 1 possible, low-significance event (LVT 151210). All BBH. (Abbott et al. 2016a,b)

# The GW era – O1



## Sept 2015 – Jan 2016: LVC O1 science run

2 high-significance ( $\text{FAR} < 1/\text{century}$ ) GW events during O1 (GW 150914, GW 151226)  
+ 1 possible, low-significance event (LVT 151210). All BBH. (Abbott et al. 2016a,b)

Sky localizations (90% credible area)

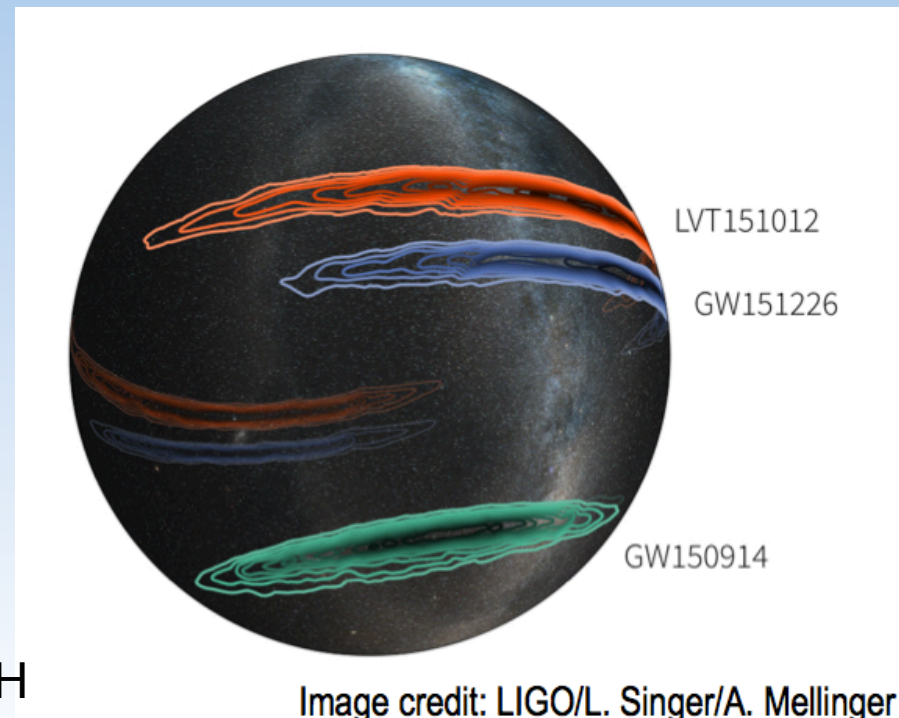
600 deg<sup>2</sup> GW 150914

1600 deg<sup>2</sup> LVT 151012

1000 deg<sup>2</sup> GW 151226

No EM counterpart found  
(despite huge observational effort)

No significant EM emission expected from BBH



# The GW era – O2



## Sept 2015 – Jan 2016: LVC O1 science run

2 high-significance (FAR < 1/century) GW events during O1 (GW 150914, GW 151226)  
+ 1 possible, low-significance event (LVT 151210). All BBH. No NS-NS / NS-BH

BBH merger rate based on O1 observations:  $9\text{-}240 \text{ Gpc}^{-3} \text{ yr}^{-1}$

NS-NS merger rate based on O1 observations:  $< 12600 \text{ Gpc}^{-3} \text{ yr}^{-1}$

NS-BH merger rate based on O1 observations:  $< 3600 \text{ Gpc}^{-3} \text{ yr}^{-1}$

(Abbott et al. 2016c,d)

# The GW era – O2



**LVC O2 run starting soon: 6 months across 2016-2017** (with a ~ 3 months stop).

~ 10 high significance (FAR < 1/century) BBH expected during O2

limits on NS-NS / NS-BH not really constraining Simulated estimates with Virgo

**Virgo will join the 2<sup>nd</sup> half of O2**

still room for EM search

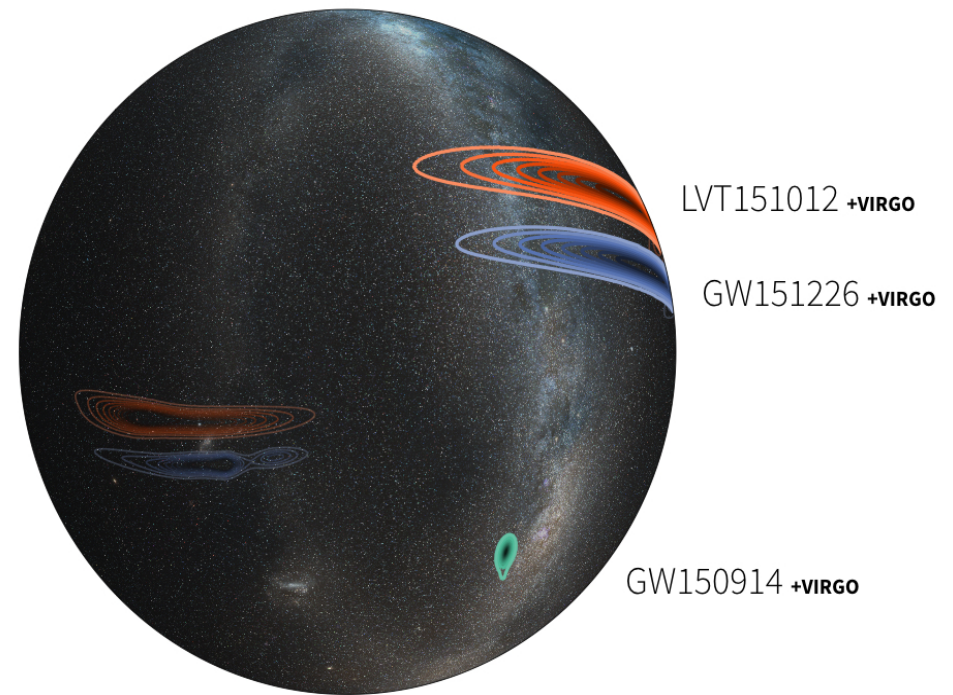


Image credit: LIGO/L. Singer/A. Mellinger

# The GW era: importance of EM detections

Precise sky localization

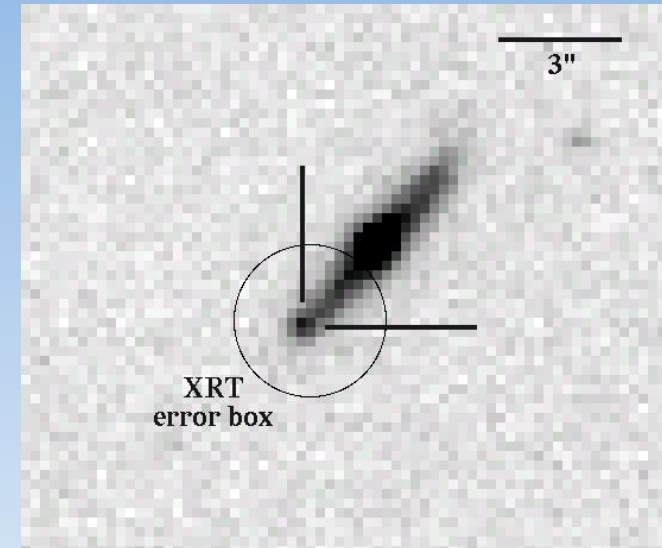
Independent measure of distance (redshift)

Luminosity & Energy

Possibility to study the environment

Constraints to the progenitor evolutionary channels

Progenitors 'smoking gun' for short GRBs





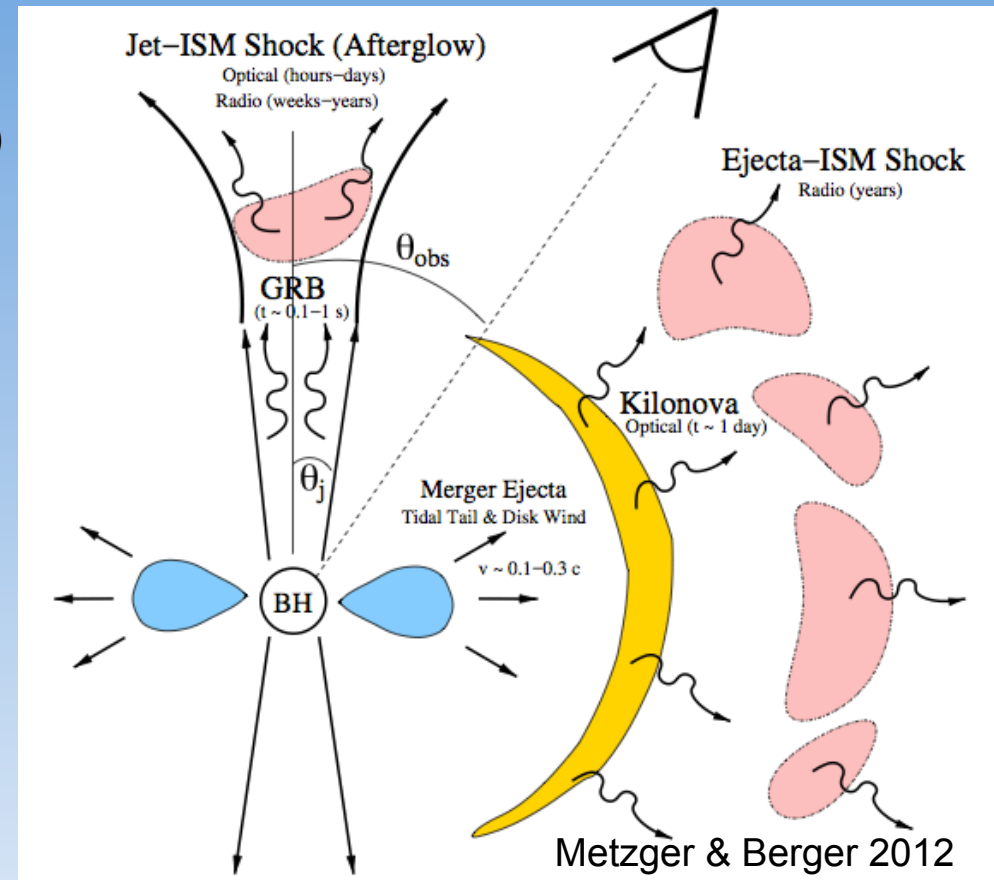
# Expected NS-NS / NS-BH EM counterparts

Short GRBs ( $\gamma$ -ray, X-ray, opt, NIR, radio)

Orphan afterglow (X-ray, opt, NIR, radio)

Macronova/Kilonova (optical, NIR)

Late-time radio remnant (radio)



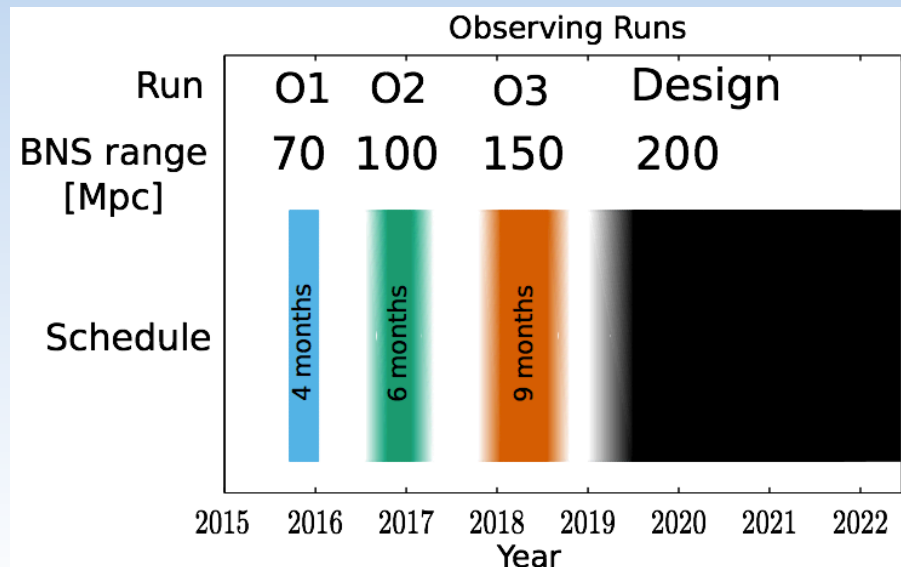
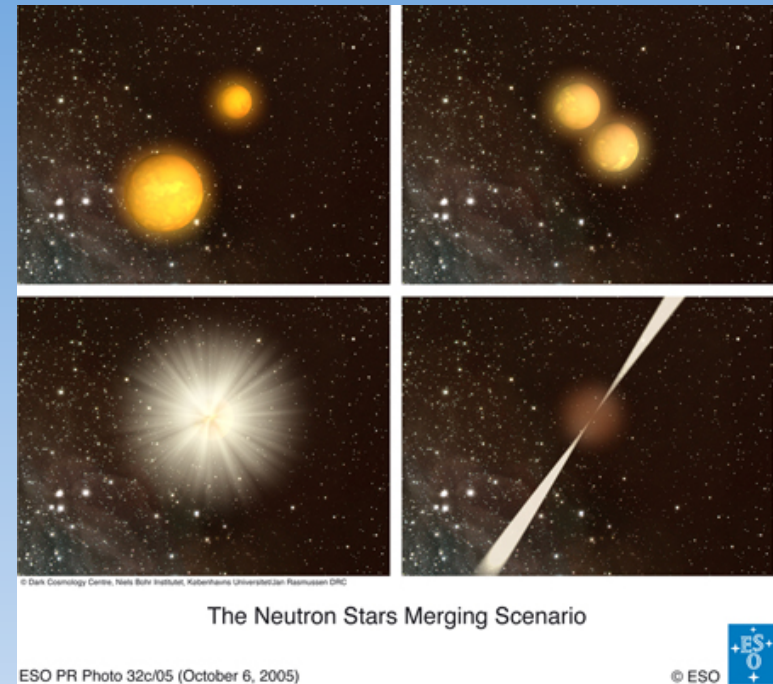
# Expected NS-NS / NS-BH EM counterparts

Short GRBs ( $\gamma$ -ray, X-ray, opt, NIR, radio)

Orphan afterglow (X-ray, opt, NIR, radio)

Macronova/Kilonova (optical, NIR)

Late-time radio remnant (radio)



How many within the LIGO-Virgo horizon?

# Short GRB rate

Current estimates of local SGRB rates range from 0.1–0.6 Gpc<sup>-3</sup> yr<sup>-1</sup> (e.g. Guetta & Piran 2005; 2006) to 1–10 Gpc<sup>-3</sup> yr<sup>-1</sup> (Guetta & Piran 2006; Guetta & Stella 2009; Coward et al. 2012; Siellez et al. 2014, Wanderman & Piran 2015) to even larger values like 40–240 Gpc<sup>-3</sup> yr<sup>-1</sup> (Nakar et al. 2006; Guetta & Piran 2006).

Rates depend on the short GRB luminosity function  $\phi(L)$  and redshift distribution  $\psi(z)$ .

# Short GRB rate

Current estimates of local SGRB rates range from 0.1–0.6 Gpc<sup>-3</sup> yr<sup>-1</sup> (e.g. Guetta & Piran 2005; 2006) to 1–10 Gpc<sup>-3</sup> yr<sup>-1</sup> (Guetta & Piran 2006; Guetta & Stella 2009; Coward et al. 2012; Siellez et al. 2014, Wanderman & Piran 2015) to even larger values like 40–240 Gpc<sup>-3</sup> yr<sup>-1</sup> (Nakar et al. 2006; Guetta & Piran 2006).

Rates depend on the short GRB luminosity function  $\phi(L)$  and redshift distribution  $\psi(z)$ .

Peak flux distribution  $\frac{dN}{dt}(P_1 < P < P_2) = \int_0^\infty dz \frac{dV(z)}{dz} \frac{\Delta\Omega_s}{4\pi} \frac{\Psi_{\text{SGRB}}(z)}{1+z} \times \int_{L(P_1, z)}^{L(P_2, z)} dL \phi(L)$

SGRB redshift distribution is a delayed star formation rate

$$\phi(L) \propto \begin{cases} (L/L_b)^{-\alpha_1} & L < L_b \\ (L/L_b)^{-\alpha_2} & L \geq L_b \end{cases}$$

The parameters of such functions are usually constrained through:

- (1) by fitting the peak flux distribution of SGRBs detected by past and/or present GRB detectors (e.g. BATSE, GBM)
- (2) the observed SGRB redshift distribution

$$\Psi(z) \propto \int_z^\infty \Psi(z') P[t(z) - t(z')] \frac{dt}{dz'} dz'$$

$$P(\tau) \propto \tau^n$$

delay time (interval between binary formation and merging) distribution function

# Selecting a complete sample of short GRBs

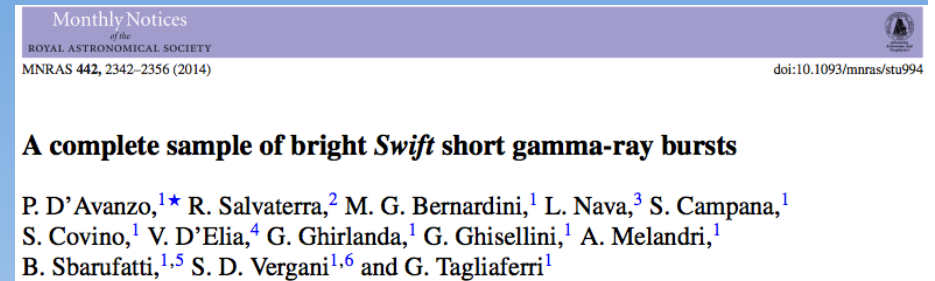
## Context:

- About 10% of the *Swift* GRBs are short
- SGRBs are fainter than long duration GRBs
- About 3/4 of SGRBs are lacking a redshift measure.

# The SBAT4: a complete sample of short GRBs

## Context:

- About 10% of the *Swift* GRBs are short
- SGRBs are fainter than long duration GRBs
- About 3/4 of SGRBs are lacking a redshift measure.



## Criteria:

- 1) Short *Swift* GRB with favorable observing conditions from the ground ( $A_V < 0.5$ ), promptly repointed by *Swift*-XRT (no need for an X-ray detection)
  - 2) Bright prompt (15-150 keV) emission (64ms peak flux  $> 3.5$  ph/cm<sup>2</sup>/s)
- 16 SGRBs (up to June 2013), 11 (69%) with redshift ( $0.12 < z < 1.30$ );  
now 27 SGRBs ~60% with redshift

**Note:** This sample is *complete* in terms of flux (it includes all the *Swift* SGRBs with  $P_{64} > 3.5$  ph/cm<sup>2</sup>/s) and, at the same time, has the highest fraction of events with measured redshift with respect to SGRBs samples presented in the literature to date.

Similar criteria were used to build the BAT6 sample of long GRBs (Salvaterra et al. 2012).

# Short GRB rate

Current estimates of local SGRB rates range from 0.1–0.6 Gpc<sup>-3</sup> yr<sup>-1</sup> (e.g. Guetta & Piran 2005; 2006) to 1–10 Gpc<sup>-3</sup> yr<sup>-1</sup> (Guetta & Piran 2006; Guetta & Stella 2009; Coward et al. 2012; Siellez et al. 2014, Wanderman & Piran 2015) to even larger values like 40–240 Gpc<sup>-3</sup> yr<sup>-1</sup> (Nakar et al. 2006; Guetta & Piran 2006).

Rates depend on the short GRB luminosity function  $\phi(L)$  and redshift distribution  $\psi(z)$ .

Peak flux distribution  $\frac{dN}{dt}(P_1 < P < P_2) = \int_0^\infty dz \frac{dV(z)}{dz} \frac{\Delta\Omega_s}{4\pi} \frac{\Psi_{\text{SGRB}}(z)}{1+z} \times \int_{L(P_1,z)}^{L(P_2,z)} dL \phi(L)$

SGRB redshift distribution is a delayed star formation rate

$$\phi(L) \propto \begin{cases} (L/L_b)^{-\alpha_1} & L < L_b \\ (L/L_b)^{-\alpha_2} & L \geq L_b \end{cases}$$

The parameters of such functions are usually constrained through:

- (1) by fitting the peak flux distribution of SGRBs detected by past and/or present GRB detectors (e.g. BATSE, GBM)
- (2) the observed SGRB redshift distribution

$$\Psi(z) \propto \int_z^\infty \Psi(z') P[t(z) - t(z')] \frac{dt}{dz'} dz'$$

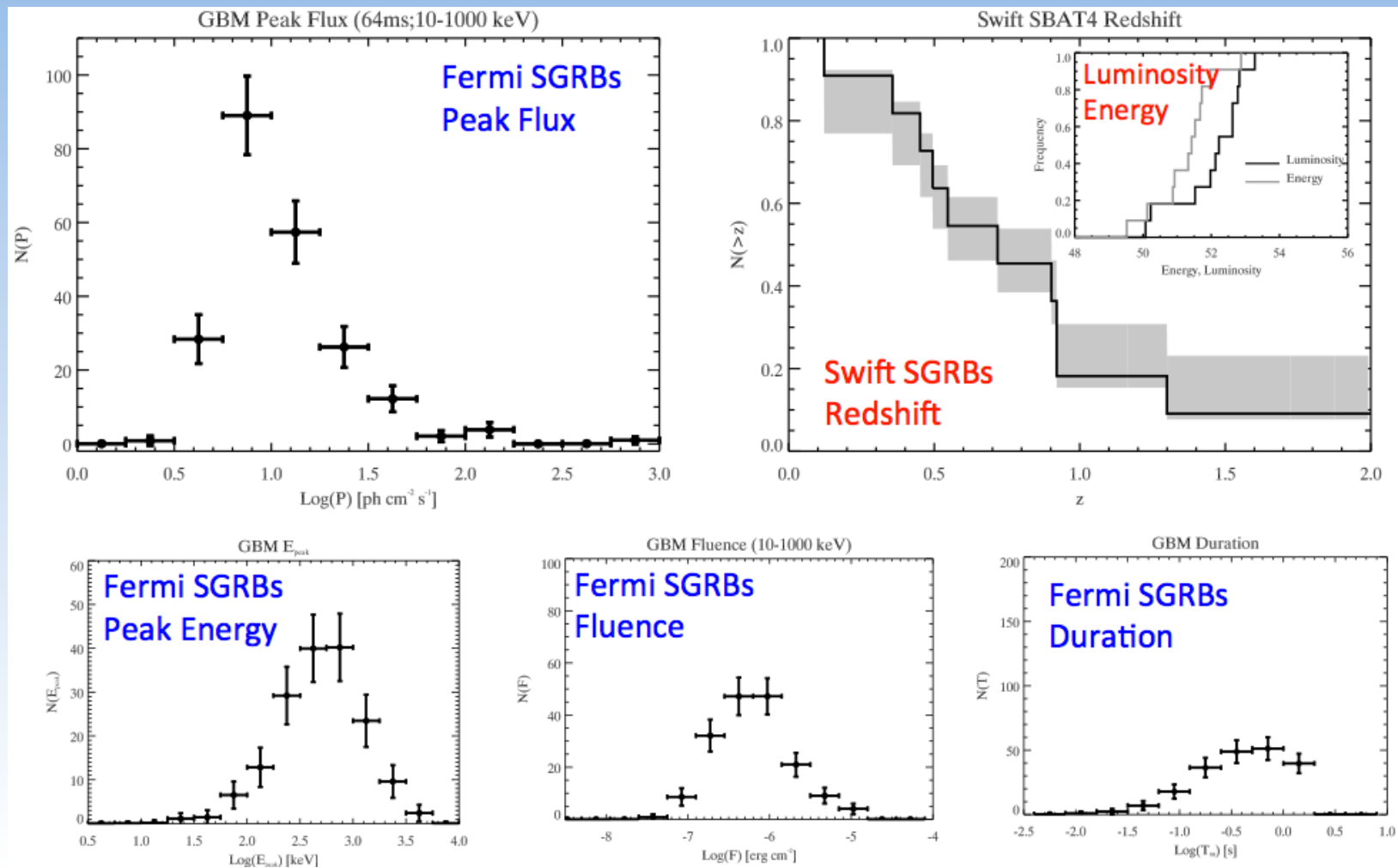
$$P(\tau) \propto \tau^n$$

delay time (interval between binary formation and merging) distribution function

# Short GRB rate: deriving luminosity function and redshift distribution

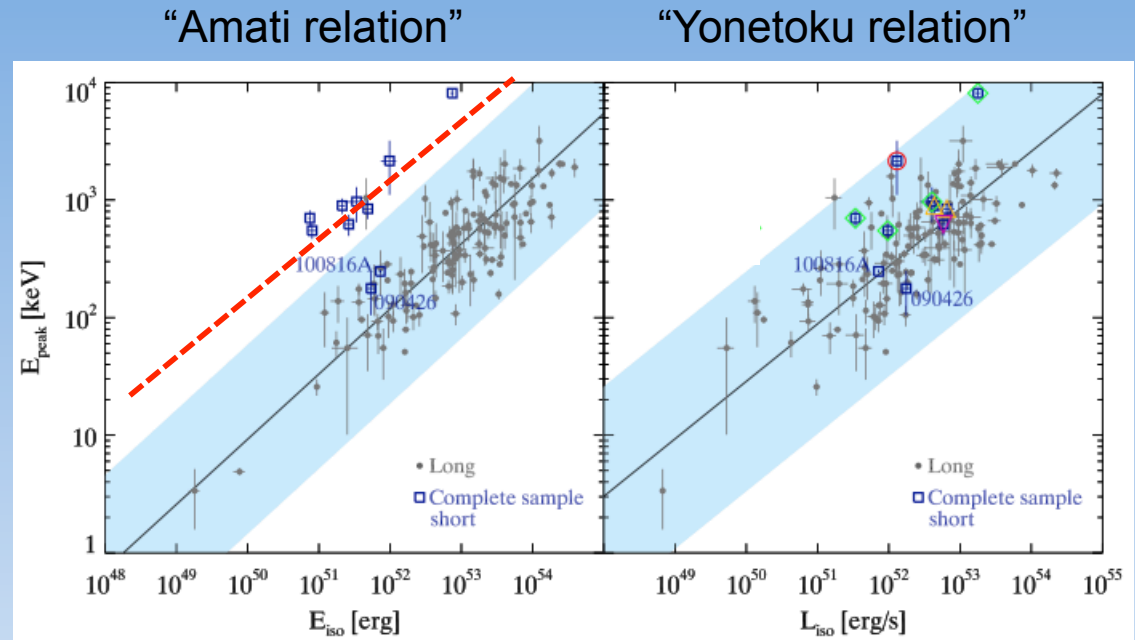
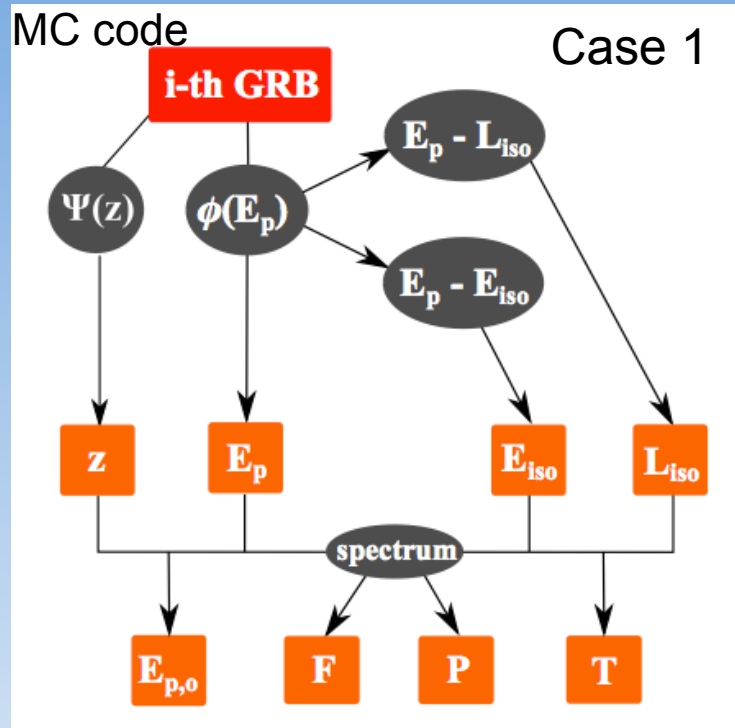
We derive the short GRB luminosity function and redshift distribution using:

- 1) all the available observer-frame constraints of the large population of bursts detected by the *Fermi*/GBM
- 2) the rest-frame properties of the *Swift* SBAT4 complete sample





# Short GRB rate: deriving luminosity function and redshift distribution



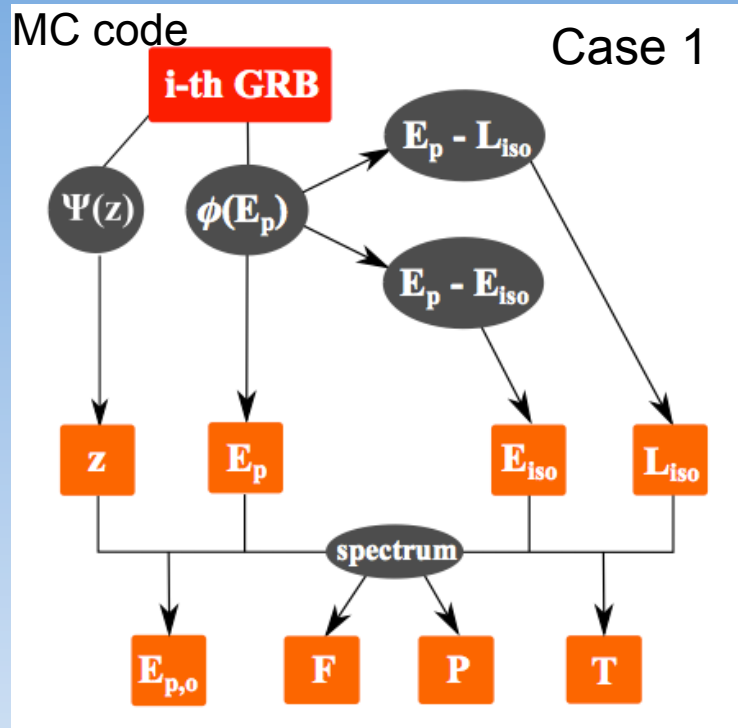
Amati et al. 2002; Yonetoku et al. 2004

$$\Psi(z) = \frac{1 + p_1 z}{1 + (z/z_p)^{p_2}}$$

$$\phi(E_p) \propto \begin{cases} \left(\frac{E_p}{E_{p,b}}\right)^{-a_1} & E_p \leq E_{p,b} \\ \left(\frac{E_p}{E_{p,b}}\right)^{-a_2} & E_p > E_{p,b} \end{cases}$$

$$T \sim 2(1+z)E/L$$

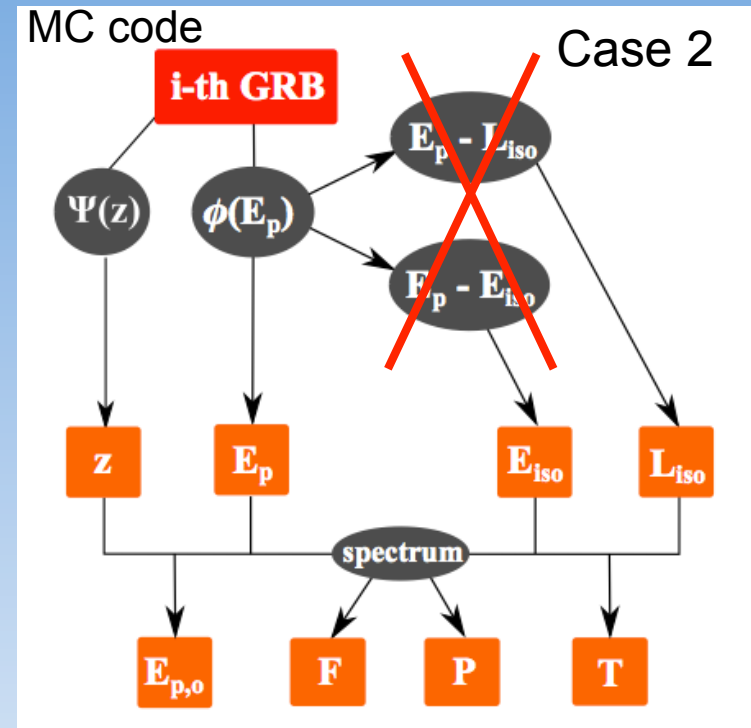
# Short GRB rate: deriving luminosity function and redshift distribution



$$\Psi(z) = \frac{1 + p_1 z}{1 + (z/z_p)^{p_2}}$$

$$\phi(E_p) \propto \begin{cases} \left(\frac{E_p}{E_{p,b}}\right)^{-a_1} & E_p \leq E_{p,b} \\ \left(\frac{E_p}{E_{p,b}}\right)^{-a_2} & E_p > E_{p,b} \end{cases}$$

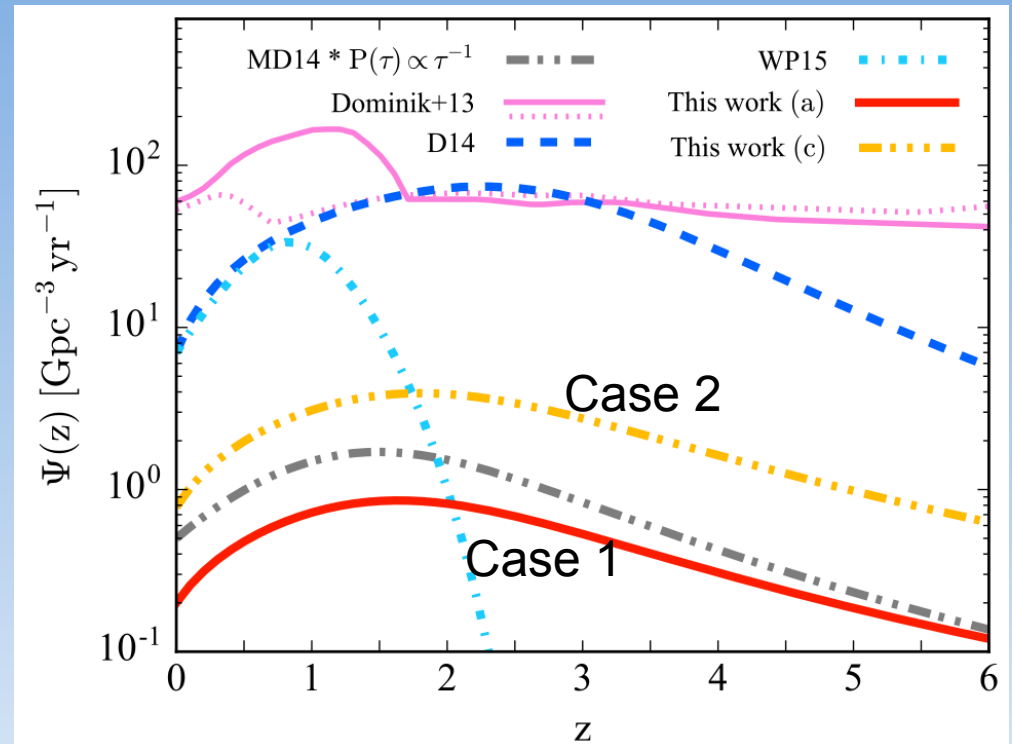
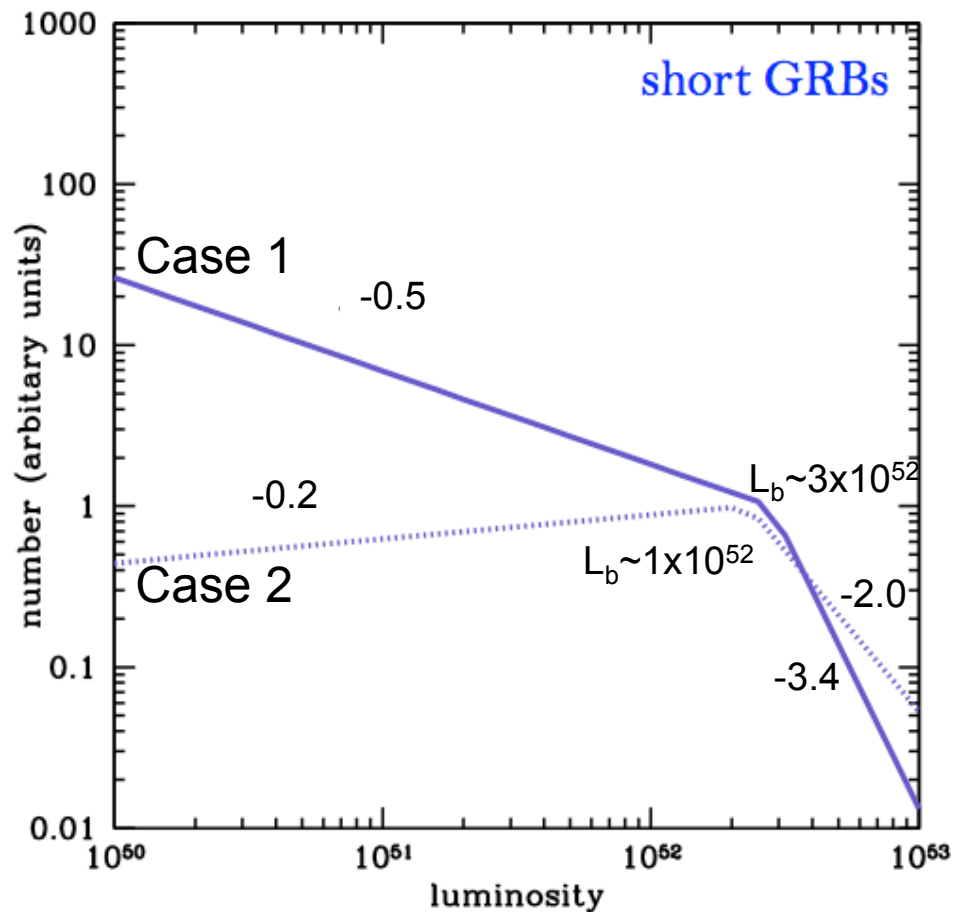
$$T \sim 2(1+z)E/L$$



$$P(L) \propto \begin{cases} (L/L_b)^{-\alpha_1} & L \leq L_b \\ (L/L_b)^{-\alpha_2} & L > L_b \end{cases}$$

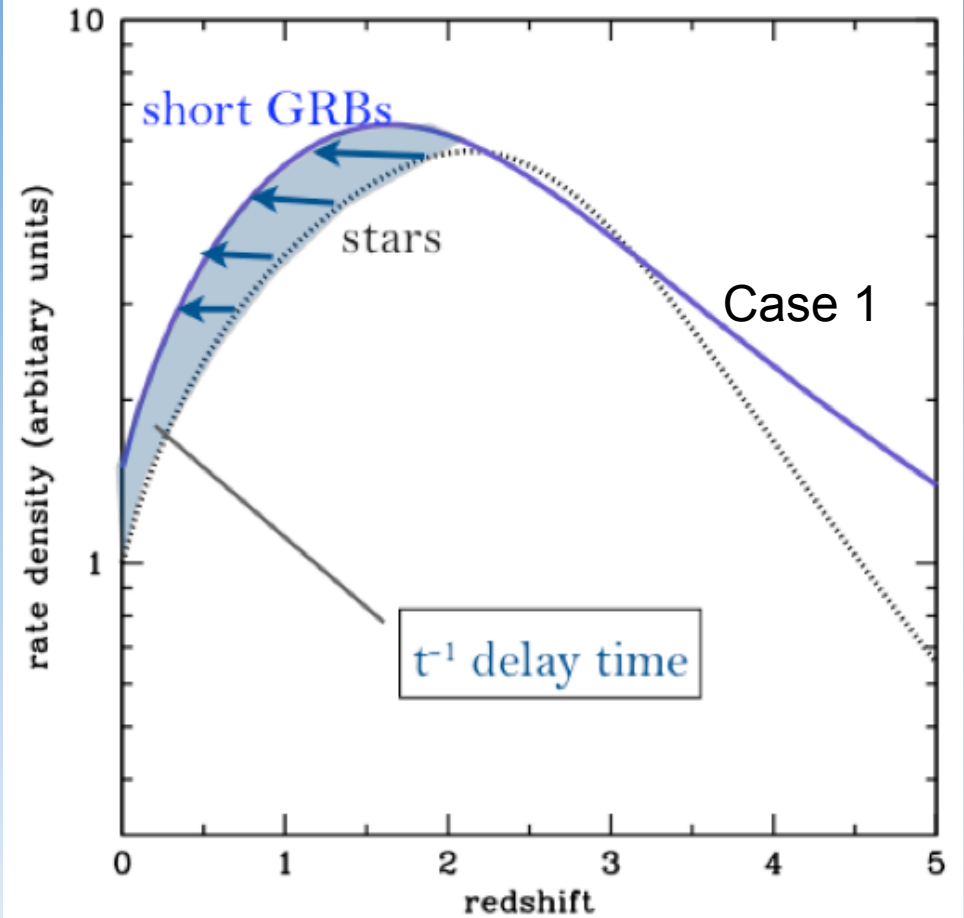
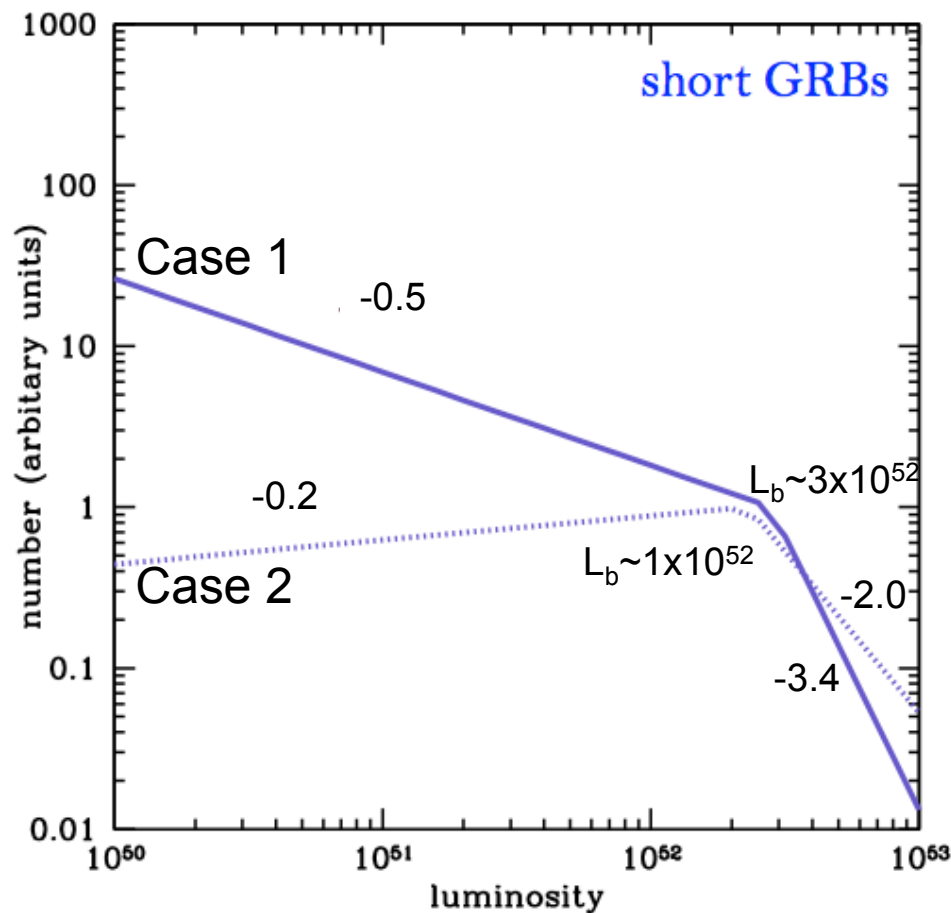
Lognormal distribution of durations

# Short GRB luminosity function and redshift distribution



$$\phi(L) \propto \begin{cases} (L/L_b)^{-\alpha_1} & L < L_b \\ (L/L_b)^{-\alpha_2} & L \geq L_b \end{cases}$$

# Short GRB luminosity function and redshift distribution

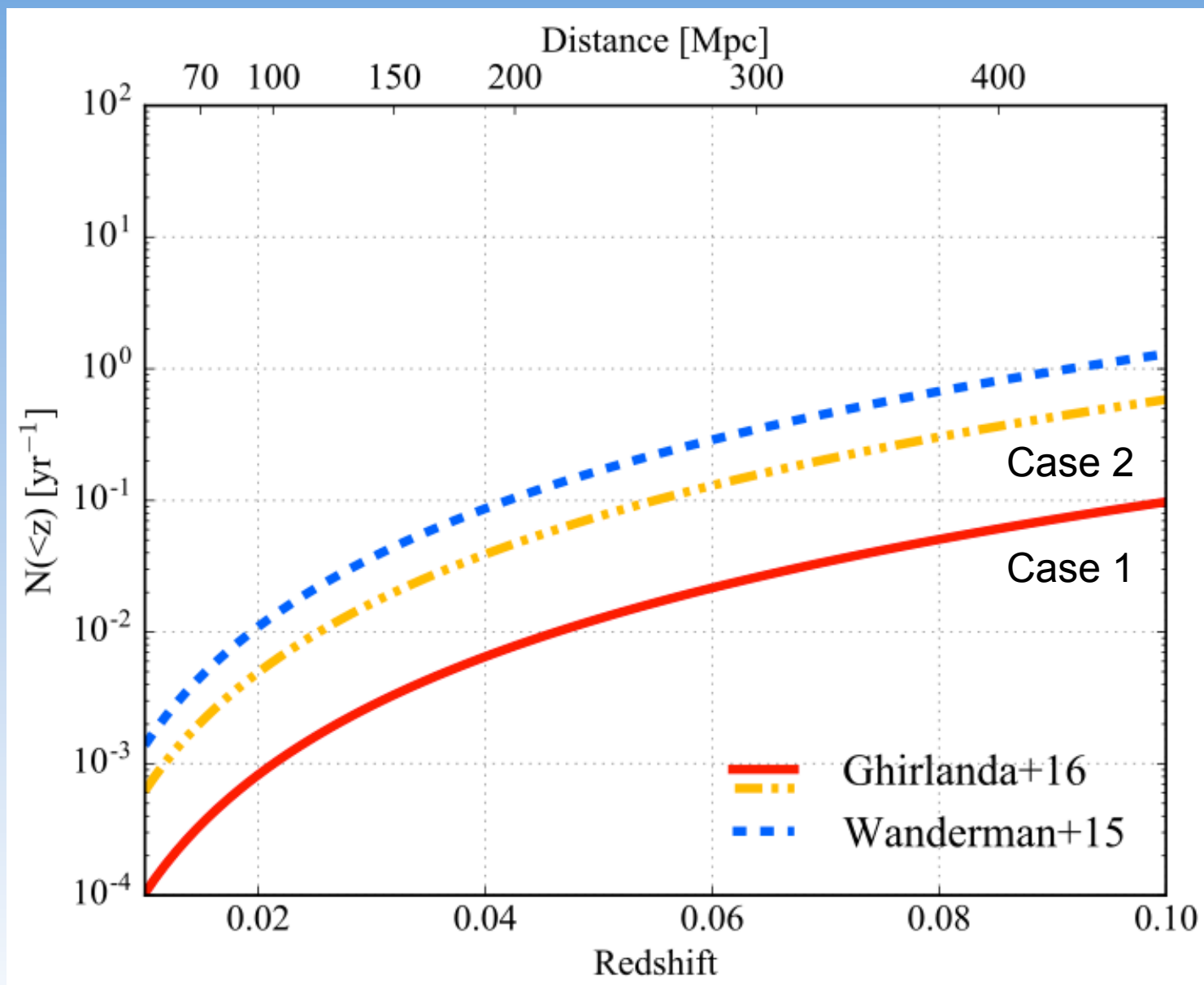


$$\phi(L) \propto \begin{cases} (L/L_b)^{-\alpha_1} & L < L_b \\ (L/L_b)^{-\alpha_2} & L \geq L_b \end{cases}$$

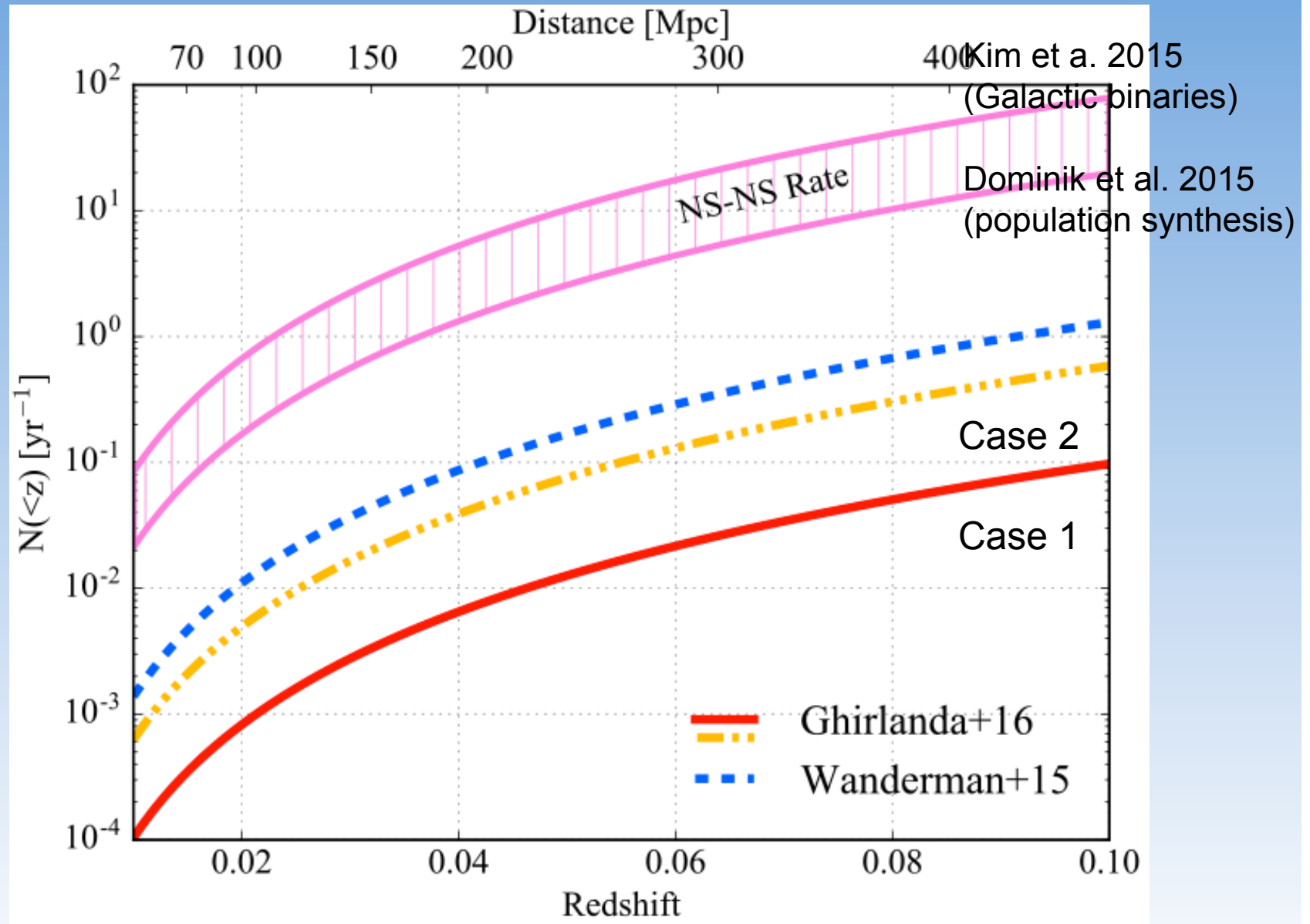
$$P(\tau) \propto \tau^{-1}$$

small delays favored; primordial binaries

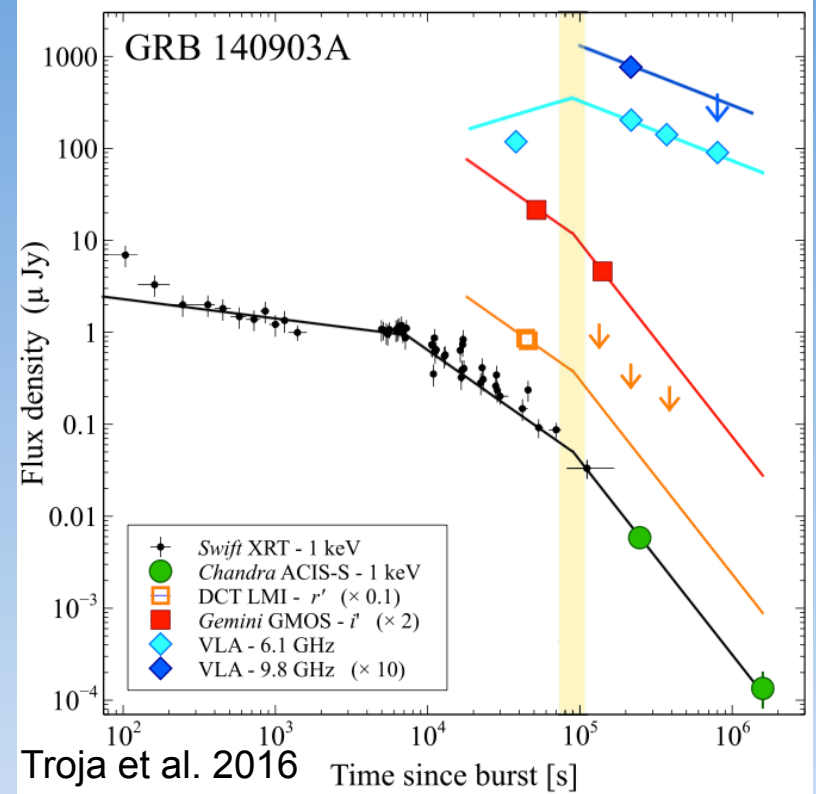
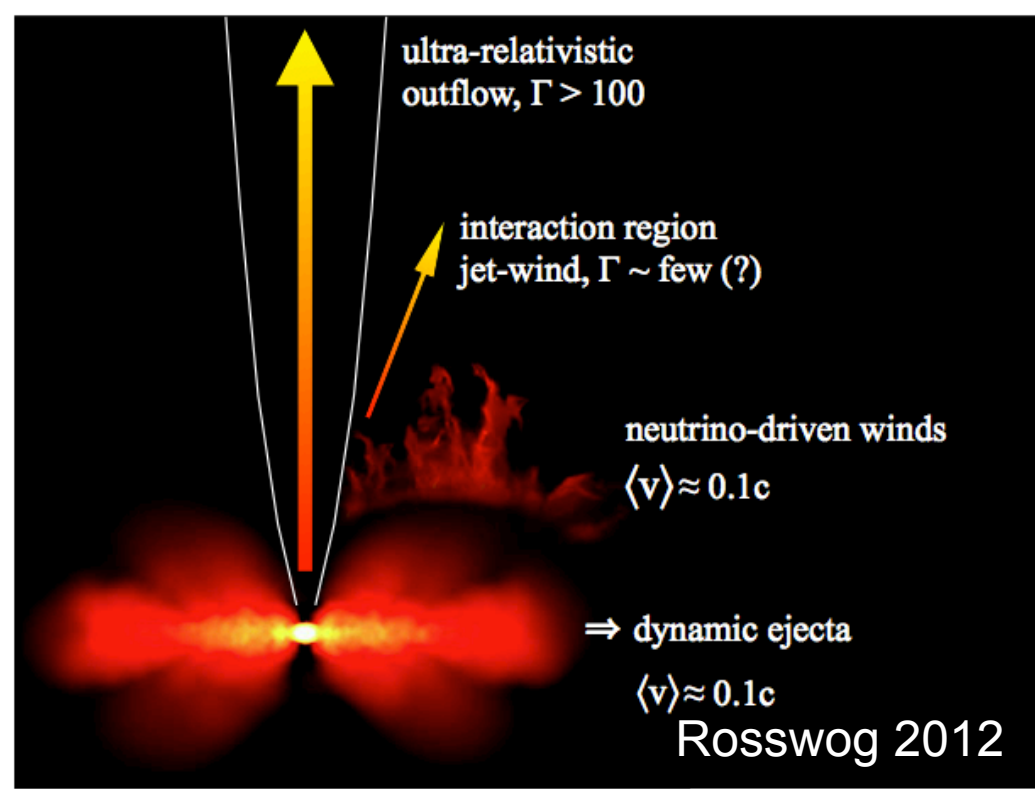
# Short GRB rate



# Short GRB rate



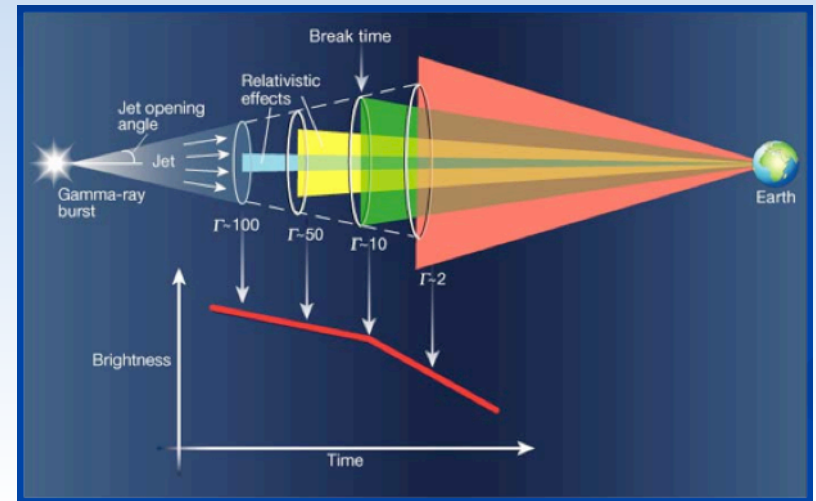
# Jets in SGRBs



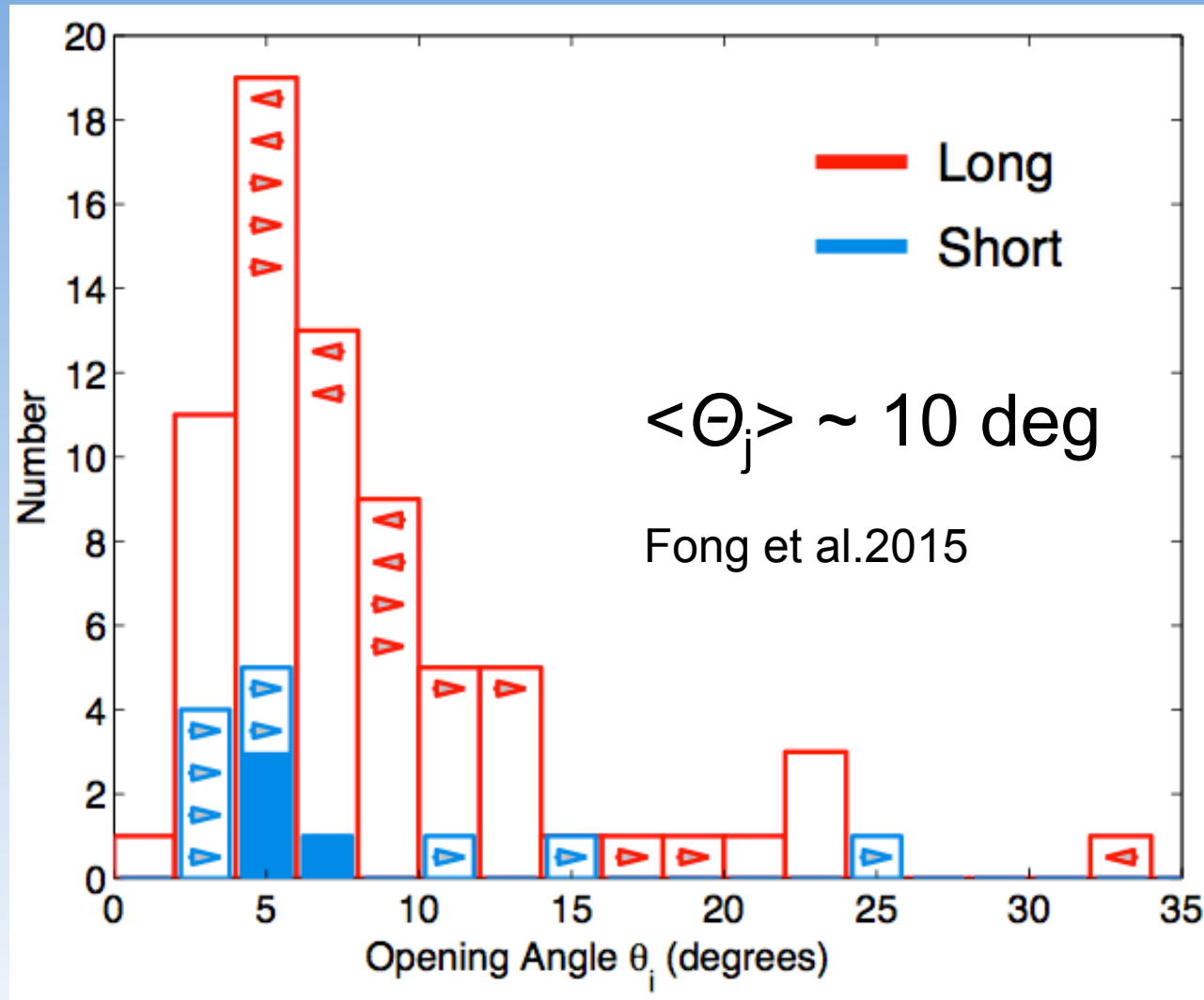
Short GRB Opening Angles

Fong et al. 2015

GRB	Band <sup>a</sup>	$\theta_j$ (deg)	$\delta t_{\text{last}}^b$ (days)	Reference
050709	O	$\gtrsim 15^\circ$	16.2	1
050724A	X	$\gtrsim 25^\circ$	22.0	2
<b>051221A</b>	X	$6-7^\circ$	26.6	3
<b>090426A</b>	O	$5-7^\circ$	2.7	4
101219A	X	$\gtrsim 4^\circ$	3.9	5, This work
<b>111020A</b>	X	$3-8^\circ$	10.2	6
111117A	X	$\gtrsim 3-10^\circ$	3.0	7, 8
120804A	X	$\gtrsim 13^\circ$	45.9	9, This work
<b>130603B</b>	OR	$4-8^\circ$	6.5	10
140903A	X	$\gtrsim 6^\circ$	3.0	11, This work
140930B	X	$\gtrsim 9^\circ$	23.1	This work



# Short GRB true rate

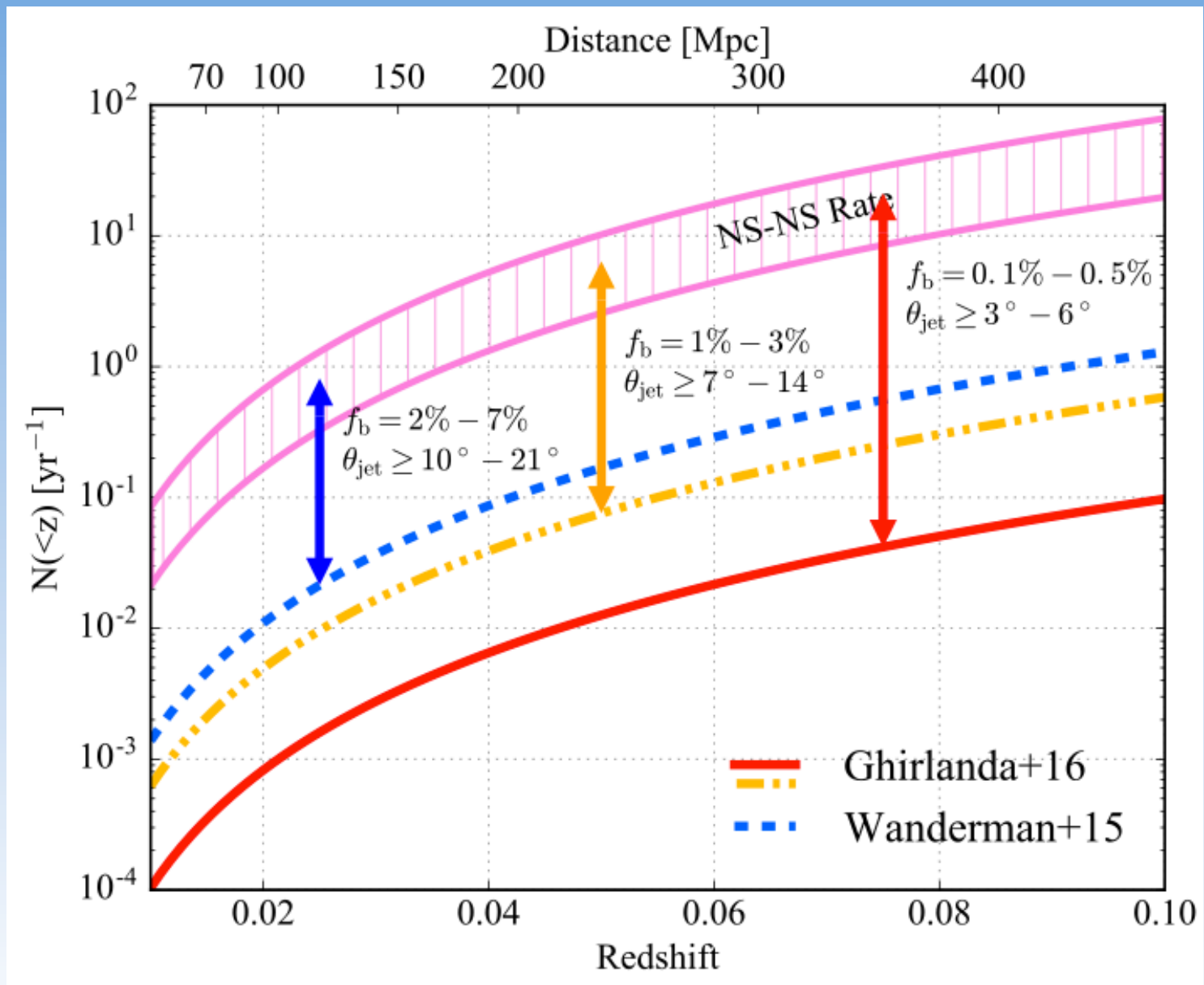


The true SGRB event rate is increased by a factor:

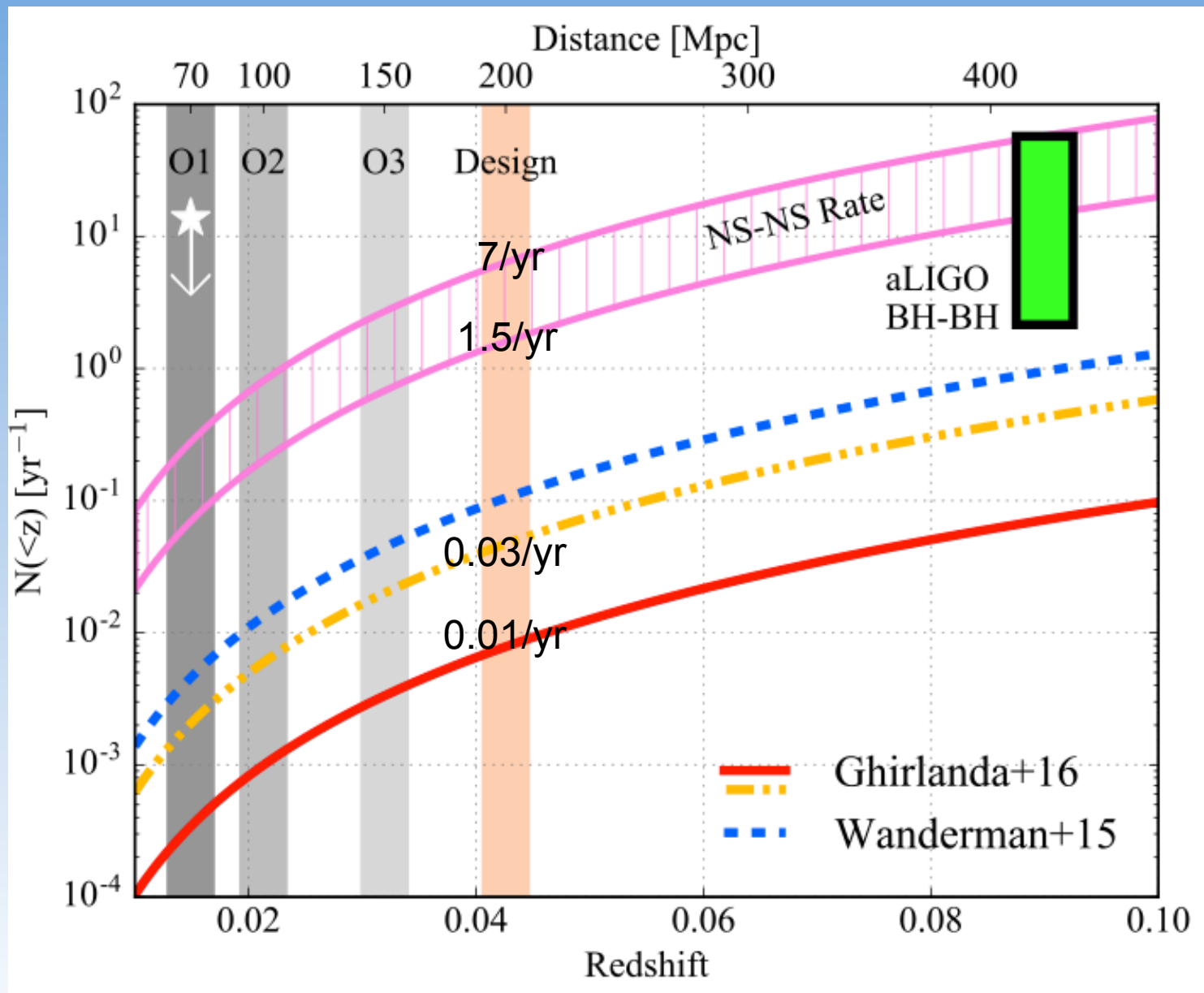
$$f_b^{-1} = (1 - \cos \Theta_j)^{-1}$$



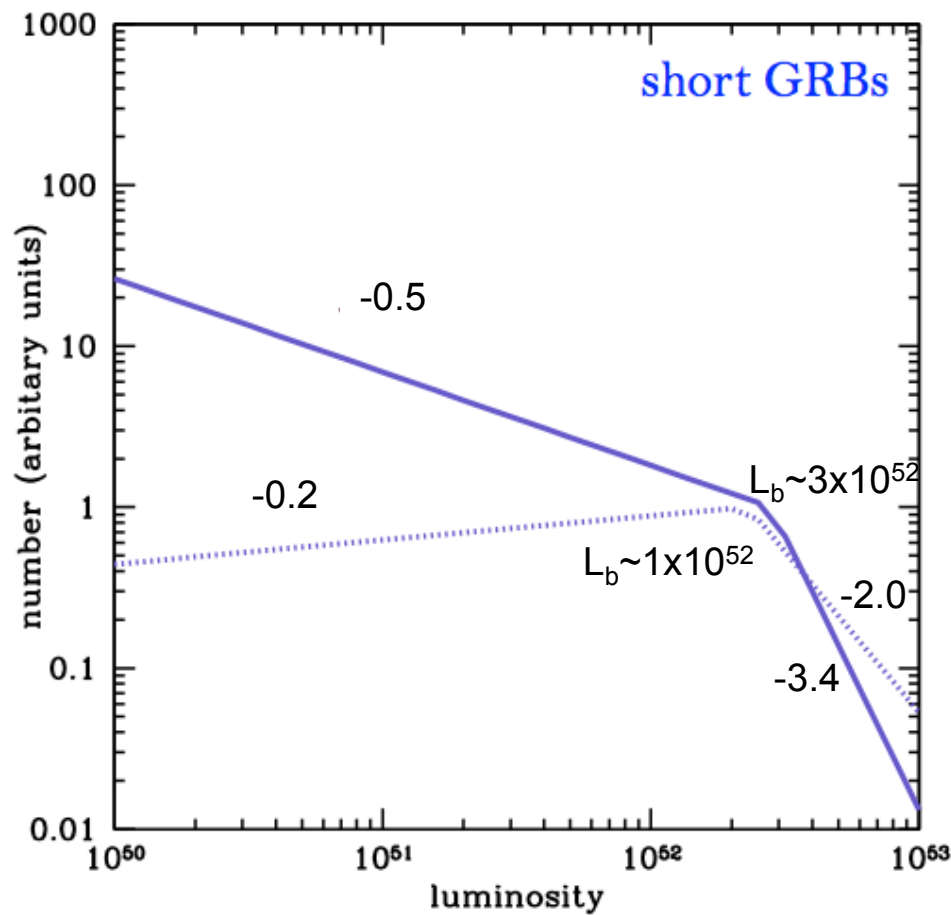
# Short GRB true rate



# Short GRB rate: forthcoming LIGO-Virgo runs



# Short GRBs luminosity function: expectations for orphan afterglows



A “flat” luminosity function implies an average Lum higher wrt a steep luminosity function

A higher prompt emission luminosity implies brighter afterglows

Good perspective for orphan afterglow detections

# Conclusions

- we derived the short GRB luminosity function, redshift distribution and local rate (within the advanced LIGO/Virgo horizon) using a large set of observational constraints
- the on-axis short GRB local (200 Mpc) rate is relatively low ( $0.01-0.03 \text{ yr}^{-1}$ )
- assuming all NS-NS mergers originate short GRBs:  $\vartheta_{\text{jet}} \sim 3-14 \text{ deg}$  (consistent with the few observations available)
- our flat luminosity function implies an average prompt emission luminosity relatively high for short GRBs: bright orphan afterglows
- waiting for the next LIGO/Virgo observing runs

Details in:

Ghirlanda et al. 2016, A&A in press, arXiv:1607.07875

D'Avanzo et al. 2014, MNRAS, 442, 2342



**Backup slides**

Rate of bursts with  
peak flux  $P_1 < P < P_2$

$$N(P_1 < P < P_2) = \frac{\Delta\Omega}{4\pi} \int_0^\infty dz \frac{dV(z)}{dz} \frac{\Psi(z)}{1+z} \int_{L(P_1,z)}^{L(P_2,z)} \phi(L) dL$$

SGRB redshift  
distribution is a  
delayed star  
formation rate

$$\Psi(z) = \int_z^\infty \psi(z') P[t(z) - t(z')] \frac{dt}{dz'} dz'$$

Delay from birth to merger

$$\phi(L) \propto \begin{cases} (L/L_b)^{-\alpha_1} & L < L_b \\ (L/L_b)^{-\alpha_2} & L \geq L_b \end{cases}$$

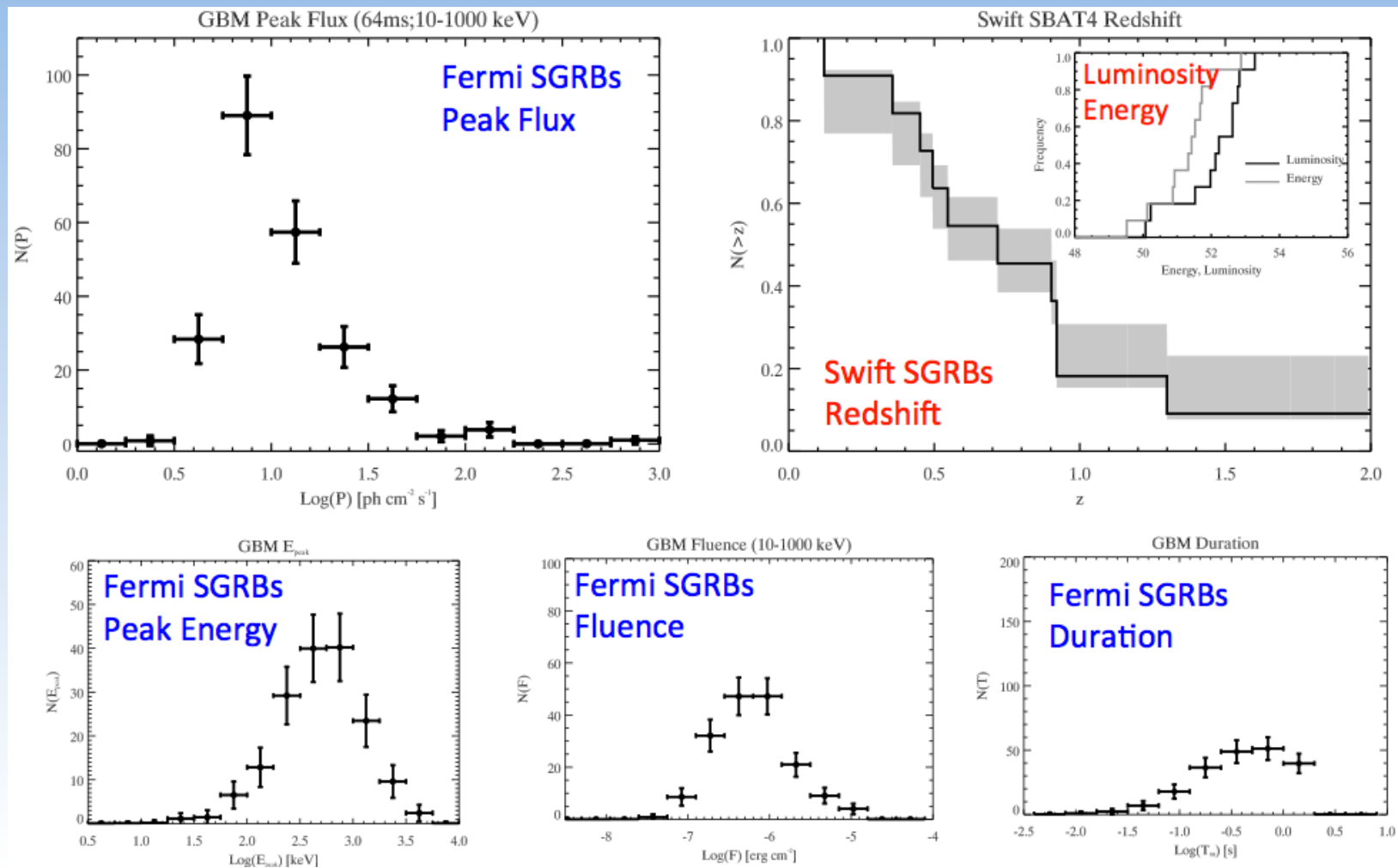
$$P(\tau) \propto \tau^n$$

delay time (interval between binary  
formation and merging) distribution  
function:

# Short GRB rate: deriving luminosity function and redshift distribution

We derive the short GRB luminosity function and redshift distribution using:

- 1) all the available observer-frame constraints of the large population of bursts detected by the *Fermi*/GBM
- 2) the rest-frame properties of the *Swift* SBAT4 complete sample





# Short GRB luminosity function and redshift distribution

